# Nanoemulsions as parenteral drug delivery systems for a new anticancer benzimidazole derivative: formulation and *in-vitro* evaluation

Rawia M. Khalil, Mona Basha, Rabab Kamel

Department of Pharmaceutical Technology, National Research Center, Cairo, Egypt

Correspondence to Mona Basha, PhD, Pharmaceutical Technology Department, National Research Center, El-Bohooth Street, 12311 Cairo, Egypt
Tel: +20 100 655 0825; fax: 0020233370931; e-mail: mona-basha@hotmail.com

**Received** 12 June 2015
**Accepted** 27 October 2015

**Egyptian Pharmaceutical Journal**
2015, 14:166–173

**Background**
Recently, much attention has been paid to the application of nanoemulsions (NEs) as drug delivery systems. Besides their high solubilization capacity, NEs are powerful carrier systems because of their thermodynamic stability, ease of preparation, and high absorption rates.
**Aim**
The present work focuses on the design of stable and dilutable NEs for intravenous administration of a potent antitumor benzimidazole derivative, a poorly water-soluble active ingredient.
**Materials and methods**
NEs were formulated using ethanol as cosurfactant and Tween 20, Acconon MCF, and Labrasol as surfactants using the oil with maximum drug solubilization. Selected NEs were evaluated for droplet size, zeta potential, morphology, *in-vitro* release profile, and physical stability.
**Results**
The results revealed the development of eight NEs composed of 10% oleic acid with an infinite dilution capacity. NE3, NE6, and NE8 having the highest surfactant to cosurfactant ratio (3: 1) showed the best drug solubilization capacity. The NE droplets appeared almost spherical, ranging from 28.21 to 153.00 nm, with narrow distribution and relatively high zeta potential. NEs demonstrated sustained release profiles, whereas increasing surfactant to cosurfactant ratio was accompanied by increased drug release. NEs showed excellent physical stability with no phase separation or change in particle size.
**Conclusion**
Our results suggest that NEs can be used as a promising intravenous delivery system.

**Keywords:**
benzimidazole derivative, cancer, *in-vitro* release, nanoemulsions, parenteral

Egypt Pharm J 14:166–173

1687-4315

## Introduction

Cancer, a serious health problem, is one of the major causes of death worldwide. The vast increase in the number of cancer patients highlights the importance and urgent need to produce safe, efficient, and promising anticancer agents [1–3]. Recently, many chemical classes of heterocyclic and fused heterocyclic compounds have been identified and evaluated for cancer therapy [4–6]. According to reported literature, benzimidazole derivatives are intensively being worked on and show remarkable biological activity as antitumor agents [7–9].

The choice of a suitable pharmaceutical formulation is clearly an essential step in the development of successful anticancer drug therapy. Challenges are generally faced during formulation because of the aqueous insolubility of certain drugs. This is crucial in the case of intravenous forms, as high concentrations of added solubilizing agents may exert severe side effects. Thus, an appropriate carrier is required to achieve a formulation of higher safety causing no venous irritation characterized by higher solubility as well as optimum stability. Among the most investigated pharmaceutical formulations, nanoemulsions (NE) have been attracting much attention owing to their several advantages [10–12]. Furthermore, these NEs guarantee controlled and sustained release of the drugs, resulting in the reduction of the dosage and frequency of injection during the drug therapy time. In addition, injectable NEs are characterized by lack of creaming, sedimentation, and flocculation in addition to large surface area and free energy, thus having prominent advantages compared with the other injectable dosage forms of larger particle size [13,14]. Moreover, the small droplet diameter of the NEs allows their sterilization using a simple and inexpensive method like filtration [15]. All of the above-mentioned remarkable



 DOI: 10.4103/1687-4315.172862

characteristics may contribute to successful intravenous administration. However, this is challenging because precipitation of incorporated drugs can occur upon dilution in blood [16,17].

In this study a parenteral delivery system was designed as a carrier for a chemically synthesized benzimidazole derivative with anticancer activity [18]. Our purpose was to develop and evaluate a suitable infinitely dilutable intravenous NE. Preliminary tests were performed on the basis of the solubilization and microemulsifying effect, together with resistance to infinite dilution, followed by evaluation and comparison of surfactants to develop oil-in-water NEs. Several NEs were formulated and segregated according to their resistance to dilution as well as surfactant and oil content. NEs resistible to dilution containing low surfactant and oil contents were selected for further evaluation, including characterization, drug solubilization capacity, *in-vitro* release study, and stability study. Further in-vivo studies related to safety and therapeutic efficacy are currently being performed.

## Materials and methods

### Materials

The drug used is a synthesized benzimidazole derivative. Labrasol (PEG-6 caprylic/capric triglycerides) and Labrafil M1944LS (decyl polyglucoside) were gift samples from Gattefosse (Saint-Priest, France). Miglyol 812 (caprylic/capric triglyceride) was kindly provided by Sasol Germany GmbH (Witten, Germany). Acconon MC8-2 (polyoxyethylene 8 caprylic/capric glycerides) was obtained as a gift sample from ABITEC Corporations (Cleveland, Ohio, USA). Isopropyl myristate, isopropyl palmitate, Tween 80 (polysorbate 80), Tween 20 (polyoxyethylene 20 sorbitan monolaurate), oleic acid (OA), ethanol, and dialysis tubing cellulose membrane (molecular weight cutoff 12 000–14 000 g/mol) were purchased from Sigma Chemical Company (St. Louis, Missouri, USA). All other chemicals used were of analytical grade.

### Methods

#### *Synthesis of benzimidazole derivative*

The drug under study was prepared by means of two steps; the first step was diazotization of 4-(1*H*-benzo[d] imidazol-2-yl)aniline (compound 1), which was achieved by using hydrochloric acid and sodium nitrite at 0 C. The second step was the reaction of the crude diazonium chloride with acetyl acetone to form compound 2. Compound 2 was reacted with hydrazine hydrate to form 4-(2-(4-(1*H*-benzo[d]imidazol-2-yl)phenyl)hydrazono)pyrazolidine-3,5-dione (compound 3), which is the drug under study [18].

#### *Screening of oils for nanoemulsions*

The solubility of the drug was determined in various oils to select the one having the best solubilizing capacity. The oils used were OA, Miglyol 812, isopropyl myristate, isopropyl palmitate, and Labrafil M1944LS. Briefly, 10 mg of drug and increasing quantities of selected oils (0.3 g every 30 min) in 10 ml glass vials were shaken at 100 rpm for 12 h in a controlled temperature water bath at 37 ± 1 C (Memmert GmbH, Schwabach, Germany). The solubility of the drug was observed visually every hour, and the amount of oil needed to give a clear solution under normal light when seen with the naked eye was recorded [19,20].

#### *Construction of pseudoternary-phase diagrams*

Pseudoternary-phase diagrams were constructed by means of the water titration method at ambient temperature. Different combinations of surfactant and cosurfactant were prepared. For each combination of surfactant and cosurfactant, three phase diagrams were constructed and the weight ratios were fixed at 1: 1, 2: 1, and 3: 1. For each phase diagram at a specific surfactant: cosurfactant (S: CoS) weight ratio, the ratios of oil to the mixture of surfactant and cosurfactant were varied: 1: 9, 2: 8, 3: 7, 4: 6, 5: 5, 6: 4, 7: 3, 8: 2, and 9: 1. Water was then added dropwise and stirred until a homogenous dispersion or solution was obtained. After each addition the system was examined visually and determined as a NE, a crude emulsion, or a gel. The endpoint of the titration was the point at which the solution becomes cloudy or turbid. On the basis of the obtained diagrams, appropriate concentrations of surfactant, cosurfactant, and oil were selected for further investigation and the preparation of drug-loaded NEs.

#### *Infinite dilution capacity*

The infinite dilution capacity of the developed systems was assessed visually according to the previously reported method [21]. One gram of each formulation was added dropwise into a beaker containing 20 ml of distilled water maintained at 37 ± 0.5 C stirred using a magnetic stirrer at 100 rpm. Only systems forming clear NEs within 1 min were selected [21].

#### *Solubility of the drug in nanoemulsions*

The solubility of the drug in prepared NEs as well as its solubility in PBS (pH 7.4) was determined. An excess amount of drug (100 mg) was added to screw-capped test tubes containing 5 ml of each NE or PBS (pH 7.4), and the mixture was mixed well for 5 min on a vortex (JULABO Labortechnik, Seelbach, Germany). The mixtures were then shaken in an isothermal shaker (37 ± 1 C) for 72 h. After reaching equilibrium, each tube was centrifuged at 9000 rpm

for 60 min, filtered through a 0.2 μm Millipore (Sigma-Aldrich, St. Louis, USA) membrane filter, appropriately diluted with ethanol, and the amount of drug determined spectrophotometrically at 292 nm.

*Preparation of drug-loaded nanoemulsions*

Depending on the constructed pseudoternary-phase diagrams and the solubility of the drug, the drug was added to the selected mixtures of oil, surfactant, and cosurfactant with varying component ratios as described previously, and then an appropriate amount of distilled water was added to the mixture dropwise and the NEs were obtained by stirring the mixtures at ambient temperature until clear, transparent systems were produced. All NEs were stored at ambient temperature.

*Characterization of the drug-loaded nanoemulsion*

*Measurement of droplet size and zeta potential*: The average droplet size, its distribution [characterized by polydispersity index (PDI)], and zeta potential of the NEs were measured using a Zetasizer Nano-ZS (Malvern Instruments, Worcestershire, UK). The measurement was taken at 25° C.

*Transmission electron microscope*: The morphology of selected NEs was investigated by transmission electron microscopy (TEM, JEM-1230; Jeol, Tokyo, Japan). A droplet of diluted NE was placed on carbon film-coated copper grids, negatively stained with a drop of 2% (w/w) phosphotungstic acid solution, and then allowed to dry for 10 min before examination on TEM.

*In-vitro drug release studies*

*In-vitro* drug release studies were conducted with the dialysis bag diffusion technique using a cellulose membrane (12 000–14 000 molecular weight cutoff). Cellulose membranes were soaked overnight in the release medium. To the preswollen cellulose membrane bags 2 ml of NE was placed, and both ends of the bags were tied. Later, dialysis bags were carefully placed in beakers containing 100 ml of PBS (pH 7.4) with 3% w/v Tween 20 (to maintain sink condition) as the release medium and the beakers were rotated at 100 rpm for 72 h at 37.0 ± 0.1° C. At specific time intervals 2 ml of the sample was drawn and replaced with an equal volume of the release medium. The amount of drug released into the medium was determined spectrophotometrically. The experiments were carried out in triplicate. To study the drug release pattern, the release data were fitted to zero, first, and second order as well as to the Higuchi model.

*Stability study*

The physical stability of the selected formulations was determined through particle size analysis, visual clarity, and phase separation. The NEs were stored at 25° C for 60 days and samples were tested at 0, 30, and 60 days of storage. The tested nanoemulsions were diluted 100 times with double-distilled water to examine their stability.

**Data analysis**

All experiments were performed three times, and the data were expressed as mean ± SD. The statistical significance of differences was determined by ANOVA using SPSS (SPSS-11; SPSS Inc., Chicago, Illinois, USA). A value of *P* less than 0.05 was considered significant.

## Results and discussion

**Screening of oils for nanoemulsions**

The safety of the selected components for intravenous administration was the primary consideration during selection. The drug may be solubilized in the oily core and/or on the interface of these structures; thus, the selected vehicles should have a good solubilizing power to the drug [22]. Therefore, the solubility of the drug in various oils was tested for proper selection of oil, and the results are presented in Table 1. On the basis of the obtained data, OA, which showed the highest solubilizing effect, was chosen for phase diagram study. The best solubilizing effect of OA was previously reported [23,24].

On preparing the NE, Tween 20, a nonionic surfactant, was chosen, reported to be safe for intravenous administration [25] and commonly used in pharmaceutical formulations [26]. Labrasol, a medium-length alkyl chain surfactant, was also selected. Labrasol had been used as a pharmaceutical excipient because of its high tolerance, low toxicity in animals, and $LD_{50}$ of 22 g/kg for rats [27], in addition to its enhancing effect on the solubilization and absorption of hydrophobic drugs [28,29]. Acconon MC8-2 is a polyoxyethylene 8 caprylic/capric glyceride. Besides its low irritancy and toxicity, ethanol being a good solvent for the drug, was chosen as the cosurfactant. Also, previous work on NE systems had shown that an ethanol cosurfactant was necessary to maintain a stable single-phase oil in

**Table 1 Screening of different oils for drug solubilization**

| Oils | Amount needed to solubilize 10 mg drug (g) |
|---|---|
| Oleic acid | 1.40 ± 0.10 |
| Labrafil M1944LS | 1.50 ± 0.20 |
| Miglyol 812 | 3.00 ± 0.20 |
| Isopropyl myristate | >6.00 |
| Isopropyl palmitate | >6.00 |

water emulsion [30]. According to earlier reports [31], the cosurfactant can lower the interfacial tension of the surfactant in NEs, resulting in a more flexible and dynamic layer. The drug in this energy-rich system can diffuse across the flexible interfacial surfactant film between the phases, a thermodynamic process that increases partitioning and diffusion. Also, it can reduce the required amount of surfactant [24].

Therefore, OA was selected as an oily core together with Tween 20, Labrasol, and Acconon MC8-2 as surfactants and ethanol as the cosurfactant. The second stage of preparing the NEs was the construction of pseudoternary-phase diagrams aiming to formulate a parenteral NE having the lowest possible surfactant content capable of optimum solubilization of the lipophilic drug used.

### Construction of pseudoternary-phase diagrams

The construction of a pseudoternary-phase diagram is essential for determining the range of concentrations and the ratios of components in the existence region of the NE. Pseudoternary-phase diagrams at different S: CoS weight ratio (1: 1, 2: 1, 3: 1) are shown in Fig. 1. As seen in all cases, compositions containing 20% oil or less showed a maximal water solubilization capacity of at least 50%. For intravenous administration, NEs should be dilutable with water without causing precipitation of the drug incorporated during clinical use [32]. Hence, the selection of appropriate surfactants is critical for preparation of o/w NE loading water-insoluble drugs.

As seen from Fig. 1, generally, the NE region relatively increased in size with the higher surfactant concentration. In group A (S: CoS is Tween 20: ethanol), the NE region somewhat increased with an increase in the S: CoS ratio from 1: 1 to 3: 1 (Fig. 1a). This could be also seen in group B (S: CoS is Labrasol: ethanol) (Fig. 1b) and group C (S: CoS is Acconon: ethanol) (Fig. 1c). This could be explained by the fact that the surfactant stabilizes the o/w interface [33]. However, this is more prominent in the case of Tween 20 (Fig. 1a) at Tween 20: ethanol (3: 1). This increase was

**Figure 1**

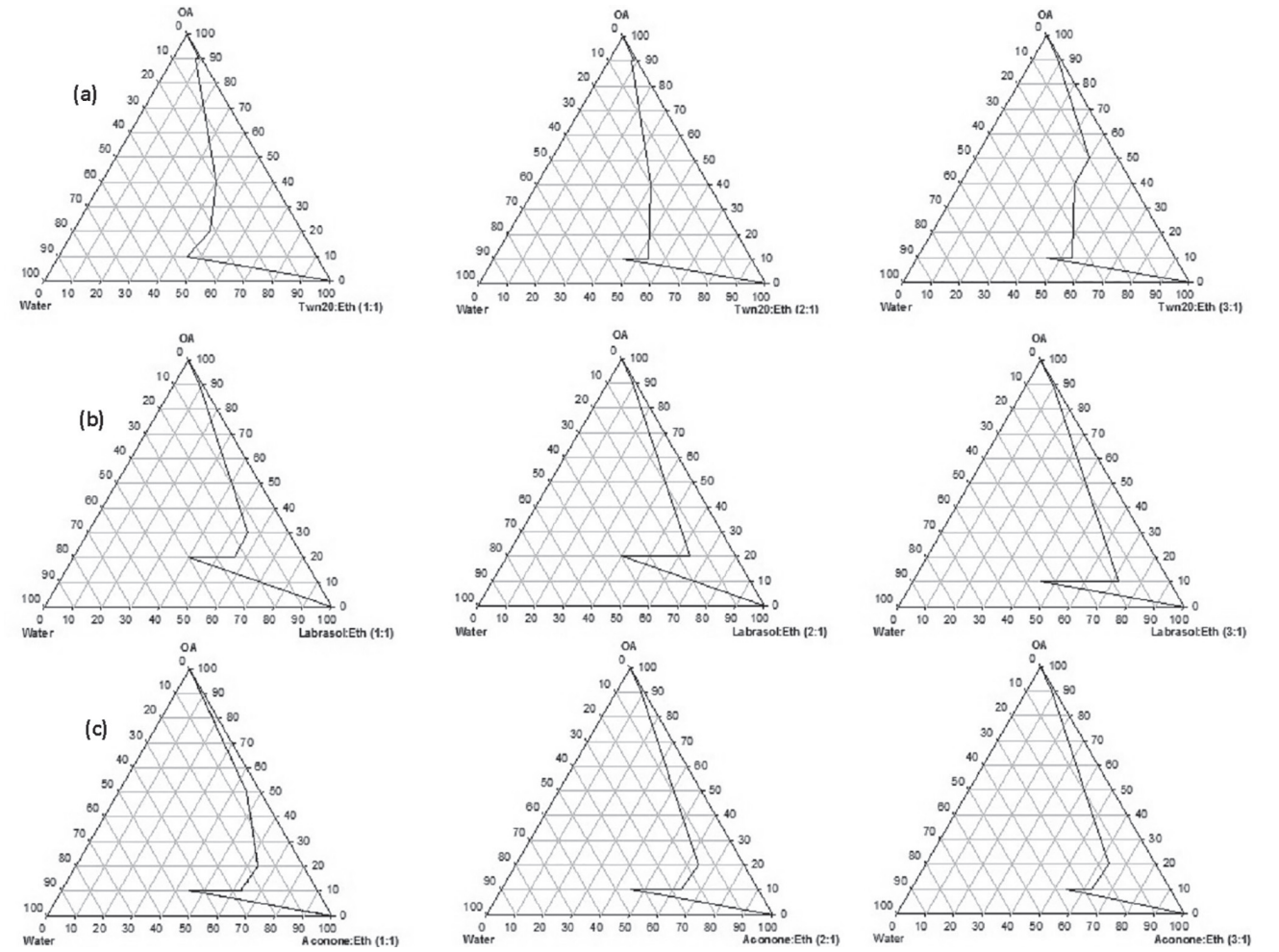


Pseudoternary-phase diagrams consisting of (a) Tween 20 (Twn20), (b) Labrasol, or (c) Acconon as surfactant, oleic acid (OA) as oil, and ethanol (Eth) as cosurfactant in different surfactant to cosurfactant ratios of 1: 1, 2: 1, and 3: 1.

toward the oil–water axis, indicating that by increasing the surfactant concentration the maximum amount of water and OA that could be solubilized into the NE increased. Therefore, we can say that the presence of more ethanol reduced the water incorporation capacity and decreased the area of the isotropic region in the phase diagrams. This agrees with the results obtained by Li *et al.* [34]. Similar results related to the increase in NE area and isotropic regions with increasing S: CoS ratio was observed by Gao *et al.* [35] as well.

### Selection of formulations

Formulation of NEs occurs at a specific concentration of oil, water, surfactant, and cosurfactant. Thus, when the NE undergoes infinite dilution upon intravenous injection, it is very probable that phase separation may occur, resulting in the precipitation of the drug owing to its poor aqueous solubility. To avoid such a situation, testing the developed NEs for dilution in double-distilled water was essential. All systems containing 10% oil or less, except for the system formed from Acconon : ethanol 1: 1, showed an infinite dilution capacity. Therefore, eight systems were selected for further investigations, the compositions of which are presented in Table 2, each composed of 50% w/w aqueous phase, 5% w/w OA, and the ratio of oil to S : CoS equal to 10 : 90. Successful systems with the least amount of oil to water (10%) were chosen because by increasing the concentration of oil the internal phase of the developed emulsion might result in progressive increase in the viscosity of the system [36], which can cause certain difficulties during intravenous administration. Upon testing for visual clarity, all prepared NEs were homogenous in shape, appearing as a transparent single-phase liquid having no traces of undissolved drug or other solid ingredients.

**Table 2 Composition of the selected nanoemulsions**

| Systems | Oil | Surfactant/cosurfactant |
|---|---|---|
| NE1 | OA | Tween 20: ethanol (1: 1) |
| NE2 | OA | Tween 20: ethanol (2: 1) |
| NE3 | OA | Tween 20: ethanol (3: 1) |
| NE4 | OA | Labrasol: ethanol (1: 1) |
| NE5 | OA | Labrasol: ethanol (2: 1) |
| NE6 | OA | Labrasol: ethanol (3: 1) |
| NE7 | OA | Acconon: ethanol (2: 1) |
| NE8 | OA | Acconon: ethanol (3: 1) |

NE, nanoemulsion; OA, oleic acid.

**Table 3 Solubility of the drug in various nanoemulsions at 37°C**

| Nanoemulsions | Drug (mg/ml) |
|---|---|
| NE1 | 0.56 ± 0.03 |
| NE2 | 0.66 ± 0.03 |
| NE3 | 0.71 ± 0.12 |
| NE4 | 0.40 ± 0.01 |
| NE5 | 0.53 ± 0.03 |
| NE6 | 0.60 ± 0.02 |
| NE7 | 0.46 ± 0.01 |
| NE8 | 0.59 ± 0.02 |

NE, nanoemulsion.

### Solubility of the drug in nanoemulsions

Being microemulsified, solubilization of the drug incorporated in the NEs may take place in the oily internal phase and/or on the interface of these systems. Both the drug loading capacity and the possibility of drug precipitation upon dilution are greatly affected by the phenomenon of drug solubilization at the interface [37]. The high loading capacity of NEs ensures a concentration gradient suitable to improve drug release [38]; therefore, testing the loading capacity (saturation solubility) of systems under investigation is necessary (Table 3).

Drug loading per formulation is a critical design factor that depends on drug solubility in various formulation components [39]. The solubility of the drug in different NE systems ranged from 0.40 ± 0.01 to 0.71 ± 0.12 mg/ml, with NE3 attaining the highest one ($P < 0.05$) compared with 0.06 ± 0.01 mg/ml, which is the solubility of the pure drug in PBS (pH 7.4). The solubility study results revealed that the drug is much more soluble in the NE systems that are capable of increasing their solubility from 6.67-fold to 11.88-fold. This observed result might be related to the use of a surfactant of higher hydrophilic-lipophilic balance (HLB) value (Tween 20 has the highest HLB = 16.7), which could enhance the continuous distribution and solubilization of the incorporated lipophilic drug within the system [40]. Focusing on NE3, NE6, and NE8 it can be noticed that generally formulations having the highest S: CoS ratio (3: 1) within a given system had the highest drug solubilization capacity because, as expected, the lower surfactant content in the NE systems decreased the solubilizing capacity of the NE [35].

### Characterization of nanoemulsions

Droplet size is one of the most representative parameters to be investigated in the evaluation of NEs and it should be ensured that they meet the requirements for intravenous administration. The results of size analysis are presented in Table 4. All NEs exhibited small droplet size and PDI, with mean values ranging from 28.21 to 205.00 nm and from 0.06 to 0.54, respectively. PDI is a measure of particle homogeneity and varies from 0.0 to 1.0. The closer the PDI values to 0, the more homogenous the particles. The small PDI of the developed NE formulations indicates the uniformity in the size distribution of the dispersed globules. NE1,

NE2, and NE3 had the smallest globule size ($P < 0.05$) compared with the other formulations (NE4–NE8). The small-sized NEs of narrow distribution suggest that they can be safely taken intravenously, passing through capillaries without causing emboli [41,42].

As shown in Table 4, the zeta potential values varied from −18.05 to −39.05 mV. It is quiet noticeable that all systems showed high zeta potential (>−30 mV) except for NE1–NE3, which had slightly lower values than the reported one (>−30 mV) required for parenteral emulsions to get full stabilization by electrostatic repulsion [43].

TEM was performed for the NE having the highest drug solubilizing power within each system (NE3, NE6, and NE8). The photomicrographs are illustrated in Fig. 2. The images show the NEs appearing as homogenous dark spots almost spherical in shape with bright surroundings.

### *In-vitro* release study

Figure 3 shows the drug release profile from different NE systems. It is obvious that within each system increasing S: CoS ratio was accompanied by subsequent increase in drug release. The systems composed of S: CoS ratio 3: 1 revealed the highest drug release profile; for example, among the NEs of group A (S: CoS is Tween 20: ethanol) NE3 attained the highest release, whereas among the NEs of group B (S: CoS is Labrasol: ethanol) NE6 showed the highest release, and NE8 in case of group C (S: CoS is Acconon: ethanol). This can be attributed to the increase in thermodynamic activity of the drug in NEs with higher concentration of surfactants [28]. The thermodynamic activity of the drug in the formulation is a significant driving force for the release. The thermodynamic driving force for release reflects the relative activities of the drug in different phases [44,45], as the drug can be released from the internal phase to the external phase and then to the release medium. As clearly illustrated in Fig. 3, among all NEs, NE6 showed the highest percentage of drug release. Besides having a S: CoS ratio of 3: 1, which results in an increase in drug release as mentioned above, NE6 is formulated using Labrasol as a surfactant, which has a well-known solubility-enhancing effect for hydrophobic drugs [28]. As shown in Table 5, all investigated NEs showed best fitting to zero-order kinetics ($R^2 \geq 0.95$), which provides an additional advantage of concentration-independent drug release pattern.

**Table 4 Characterization of nanoemulsions**

| Systems | Particle size (nm) | PDI | Zeta potential (mV) |
|---|---|---|---|
| NE1 | 35.26 ± 3.66 | 0.381 ± 0.006 | −20.80 ± 0.00 |
| NE2 | 28.21 ± 0.00 | 0.538 ± 0.026 | −18.05 ± 1.48 |
| NE3 | 26.29 ± 2.72 | 0.331 ± 0.001 | −21.85 ± 1.20 |
| NE4 | 153.00 ± 15.84 | 0.238 ± 0.018 | −39.05 ± 2.05 |
| NE5 | 114.05 ± 11.81 | 0.211 ± 0.011 | −30.45 ± 0.92 |
| NE6 | 122.40 ± 0.00 | 0.086 ± 0.019 | −35.30 ± 0.28 |
| NE7 | 116.55 ± 8.27 | 0.222 ± 0.024 | −35.65 ± 0.35 |
| NE8 | 153.00 ± 15.84 | 0.062 ± 0.017 | −33.15 ± 0.64 |

NE, nanoemulsion; PDI, polydispersity index.

**Figure 2**

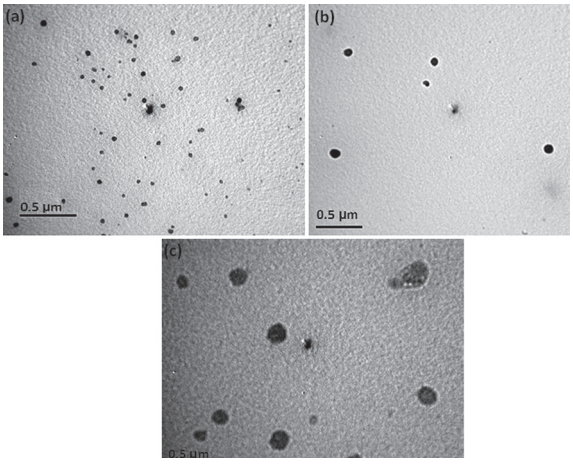


Transmission electron microphotography of NE3, NE6, and NE8. NE, nanoemulsion.

### Stability study

Stability studies of the selected NE formulations were performed by subjecting them to visual inspection and particle size analysis for 60 days. As illustrated in Fig. 4, all tested formulations showed a nonsignificant change in size ($P < 0.05$) over the studied period. Moreover, visual inspection revealed that the NEs remained stable, showing no precipitation or phase separation and remained resistable to dilution over the period of stability testing.

**Figure 3**

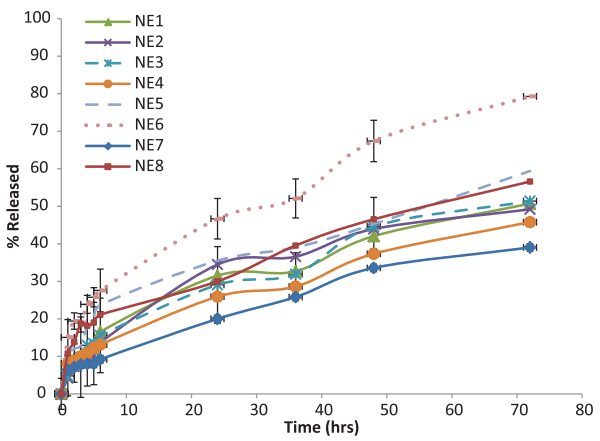


Release profiles of the drug from nanoemulsions (NE).

**Table 5 Release parameters of nanoemulsions**

| Formula | Zero order | Higuchi | First order |
|---|---|---|---|
| NE1 | | | |
| $R^2$ | 0.9577 | 0.85 | 0.8807 |
| Rate | 0.7228 | 4.3226 | 0.0151 |
| NE2 | | | |
| $R^2$ | 0.98 | 0.8453 | 0.8561 |
| Rate | 0.8304 | 4.896 | 0.0185 |
| NE3 | | | |
| $R^2$ | 0.9625 | 0.8736 | 0.8069 |
| Rate | 0.7482 | 4.5251 | 0.016 |
| NE4 | | | |
| $R^2$ | 0.9839 | 0.8213 | 0.9349 |
| Rate | 0.6038 | 3.5018 | 0.0136 |
| NE5 | | | |
| $R^2$ | 0.9474 | 0.8922 | 0.8503 |
| Rate | 0.7245 | 4.4634 | 0.0124 |
| NE6 | | | |
| $R^2$ | 0.9746 | 0.8599 | 0.9008 |
| Rate | 1.0245 | 6.1089 | 0.0122 |
| NE7 | | | |
| $R^2$ | 0.9985 | 0.7588 | 0.9734 |
| Rate | 0.5742 | 3.1776 | 0.0155 |
| NE8 | | | |
| $R^2$ | 0.9671 | 0.8682 | 0.8686 |
| Rate | 0.6809 | 4.0952 | 0.0111 |

NE, nanoemulsion.

**Figure 4**

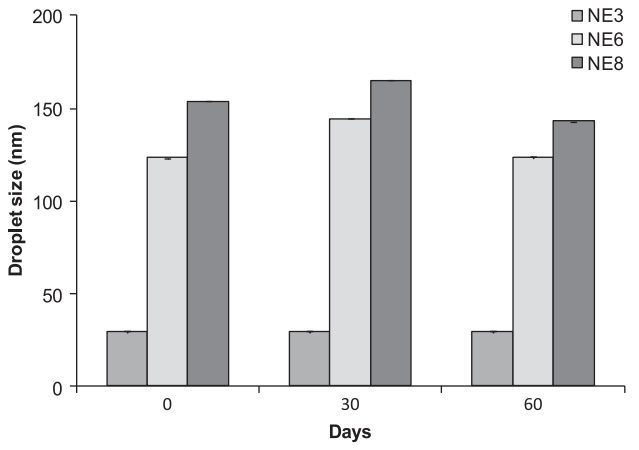


Droplet size (nm) of NE3, NE6, and NE8 formulations measured at 0, 30, and 60 days of storage at room temperature.

## Conclusion

This study showed the feasibility of preparation of safe, stable, and infinitely dilutable NEs as a suitable intravenous delivery system for the drug under study, enhancing its solubility and showing a concentration-independent drug release pattern.

### Acknowledgements

The authors thank Professor Dr Hoda I. El Diwani, Assistant Professor Shadia A. Galal, and Muhammad K.F. Khattab, Department of Chemistry of Natural and Microbial Products, Division of Pharmaceutical and Drug Industries Research, National Research Centre (Cairo, Egypt) for providing the drug under study. The authors also thank the Project's Sector at NRC (Egypt) for funding this study through project fund number 9100104.

### Financial support and sponsorship

Nil.

### Conflicts of interest

There are no conflicts of interest.

## References

1. Rashid M, Husain A, Shaharyar M, Mishra R, Hussain A, Afzal O. Design and synthesis of pyrimidine molecules endowed with thiazolidin-4-one as new anticancer agents. Eur J Med Chem, 2014; 83:630–645.
2 Grosse S, Mathieu V, Pillard C, Massip S, Marchivie M, Jarry C, *et al.* New imidazo[1,2-b]pyrazoles as anticancer agents: synthesis, biological evaluation and structure activity relationship analysis. Eur J Med Chem 2014; 84:718–730.
3 Stewart DJ, Batist G. Redefining cancer: a new paradigm for better and faster treatment innovation. J Popul Ther Clin Pharmacol 2014; 21:e56–e65.
4 Meng LH, Liao ZY, Pommier Y. Non-camptothecin DNA topoisomerase I inhibitors in cancer therapy. Curr Top Med Chem 2003; 3:305–320.
5 Pommier Y. Topoisomerase I inhibitors: camptothecins and beyond. Nat Rev Cancer 2006; 6:789–802.
6 Demirayak S, Abu Mohsen U, Cagri Karaburun A. Synthesis and anticancer and anti-HIV testing of some pyrazino[1,2-a]benzimidazole derivatives. Eur J Med Chem 2002; 37:255–260.
7 Coban G, Zencir S, Zupkó I, Réthy B, Gunes HS, Topcu Z. Synthesis and biological activity evaluation of 1H-benzimidazoles via mammalian DNA topoisomerase I and cytostaticity assays. Eur J Med Chem 2009; 44:2280–2285.
8 Singh M, Tandon V. Synthesis and biological activity of novel inhibitors of topoisomerase I: 2-aryl-substituted 2-bis-1H-benzimidazoles. Eur J Med Chem 2011; 46:659–669.
9 Alpan AS, Gunes HS, Topcu Z. 1H-Benzimidazole derivatives as mammalian DNA topoisomerase I inhibitors. Acta Biochim Pol 2007; 54:561–565.
10 Gan L, Gan Y, Zhu C, Zhang X, Zhu J. Novel microemulsion in situ electrolyte-triggered gelling system for ophthalmic delivery of lipophilic cyclosporine A: *in vitro* and *in vivo* results. Int J Pharm 2009; 365:143–149.
11 Tsai YH, Hsieh YH, Huang YB, Chang JS, Huang CT, Wu PC. Microemulsions for intravesical delivery of gemcitabine. Chem Pharm Bull (Tokyo) 2010; 58:1461–1465.
12 Wu PC, Lin YH, Chang JS, Huang YB, Tsai YH. The effect of component of microemulsion for transdermal delivery of nicardipine hydrochloride. Drug Dev Ind Pharm 2010; 36:1398–1403.
13 Patel R, Patel KP. Advances in novel parenteral drug delivery systems. Asian J Pharm 2010; 4:193–199.
14 Ravi Theaj Prakash U, Thiagarajan P. Nanoemulsions for drug delivery through different routes. Res Biotechnol 2011; 2:1–13.
15 Darole PS, Hegde DD, Nair HA. Formulation and evaluation of microemulsion based delivery system for amphotericin B. AAPS PharmSciTech 2008; 9:122–128.
16 Nornoo AO, Chow DS. Cremophor-free intravenous microemulsions for paclitaxel II. Stability, *in vitro* release and pharmacokinetics. Int J Pharm 2008; 349:117–123.
17 Nornoo AO, Osborne DW, Chow DS. Cremophor-free intravenous microemulsions for paclitaxel I: formulation, cytotoxicity and hemolysis. Int J Pharm 2008; 349:108–116.
18 Abdelgawad MA, Kamel GM. Synthesis of novel derivatives of benzothiazole and benzothiazole isosters of expected activity against breast cancer. Beni-Suef Univ J Appl Sci 2012; 2:80–88.

**19** Nikolic S, Keck CM, Anselmi C, Muller RH. Skin photoprotection improvement: synergistic interaction between lipid nanoparticles and organic UV filters. Int J Pharm 2011; 414:276–284.

**20** Kamel R, Basha M. Preparation and *in vitro* evaluation of rutin nanostructured liquisolid delivery system. Bull Fac Pharm 2013; 51:261–272.

**21** Khoo SM, CJ Porter, WN Charman. Formulation design and bioavailability assessment of lipidic self-emulsifying formulations of halofantrine. Int J Pharm 1998; 167:155–164.

**22** Hu L, Wu H, Niu F, Yan C, Yang X, Jia Y. Design of fenofibrate microemulsion for improved bioavailability. Int J Pharm 2011; 420:251–255.

**23** Chen H, Chang X, Du D, Li J, Xu H, Yang X. Microemulsion-based hydrogel formulation of ibuprofen for topical delivery. Int J Pharm 2006; 315(1-2): 52–58.

**24** Yuan Y, Li SM, Mo FK, Zhong DF. Investigation of microemulsion system for transdermal delivery of meloxicam. Int J Pharm 2006; 321:117–123.

**25** Park KM, Kim CK. Preparation and evaluation of flurbiprofen-loaded microemulsion for parenteral delivery. Int J Pharm 1999; 181: 173–179.

**26** Gursoy RN, Benita S. Self-emulsifying drug delivery systems (SEDDS) for improved oral delivery of lipophilic drugs. Biomed Pharmacother 2004; 58:173–182.

**27** Sha X, Yan G, Wu Y, Li J, Fang X. Effect of self-microemulsifying drug delivery systems containing Labrasol on tight junctions in Caco-2 cells. Eur J Pharm Sci 2005; 24:477–486.

**28** Rhee YS, Choi JG, Park ES, Chi SC. Transdermal delivery of ketoprofen using microemulsions. Int J Pharm 2001; 228:161–170.

**29** Zhang Q, Jiang X, Jiang W, Lu W, Su L, Shi Z. Preparation of nimodipine-loaded microemulsion for intranasal delivery and evaluation on the targeting efficiency to the brain. Int J Pharm 2004; 275:85–96.

**30** Lee PJ, Langer R, Shastri VP. Novel microemulsion enhancer formulation for simultaneous transdermal delivery of hydrophilic and hydrophobic drugs. Pharm Res 2003; 20:264–269.

**31** Trotta M, Gallarate M, Pattarino F, Carlotti ME. Investigation of the phase behaviour of systems containing lecithin and 2-acyl lysolecithin derivatives. Int J Pharm 1999; 190:83–89.

**32** Lawrence MJ, Rees GD. Microemulsion-based media as novel drug delivery systems. Adv Drug Deliv Rev 2000; 45:89–121.

**33** Levy MY, Polacheck I, Barenholz Y, Benita S. Efficacy evaluation of a novel submicron miconazole emulsion in a murine cryptococcosis model. Pharm Res 1995; 12:223–230.

**34** Li L, Nandi I, Kim KH. Development of an ethyl laurate-based microemulsion for rapid-onset intranasal delivery of diazepam. Int J Pharm 2002; 237:77–85.

**35** Gao Y, Wang Y, Ma Y, Yu A, Cai F, Shao W, Zhai G. Formulation optimization and in situ absorption in rat intestinal tract of quercetin-loaded microemulsion. Colloids Surf B Biointerfaces 2009; 71:306–314.

**36** Nazar MF, Khan AM, Shah SS. Microemulsion system with improved loading of piroxicam: a study of microstructure. AAPS PharmSciTech 2009; 10:1286–1294.

**37** Narang AS, Delmarre D, Gao D. Stable drug encapsulation in micelles and microemulsions. Int J Pharm 2007; 345:9–25.

**38** Kreilgaard M, Pedersen EJ, Jaroszewski JW. NMR characterisation and transdermal drug delivery potential of microemulsion systems. J Control Release 2000; 69:421–433.

**39** Subramanian N, Ray S, Ghosal SK, Bhadra R, Moulik SP. Formulation design of self-microemulsifying drug delivery systems for improved oral bioavailability of celecoxib. Biol Pharm Bull 2004; 27:1993–1999.

**40** Tsai YH, Lee KF, Huang YB, Huang CT, Wu PC. *In vitro* permeation and *in vivo* whitening effect of topical hesperetin microemulsion delivery system. Int J Pharm 2010; 388:257–262.

**41** Driscoll DF, Bhargava HN, Li L, Zaim RH, Babayan VK, Bistrian BR. Physicochemical stability of total nutrient admixtures. Am J Health Syst Pharm 1995; 52:623–634.

**42** Singh M, Ravin, LJ. Parenteral emulsions as drug carrier system. J Parenter Sci Technol 1986; 40:34–41.

**43** Müller RH, Heinemann S. Fat emulsions for parenteral nutrition. I: Evaluation of microscopic and laser light scattering methods for the determination of the physical stability. Clin Nutr 1992; 11:223–236.

**44** Delgado-Charro MB. Iontophoretic drug delivery across the nail. Expert Opin Drug Deliv 1997; 9:91–103.

**45** Delgado-Charro MB, Guy RH. Transdermal reverse iontophoresis of valproate: a noninvasive method for therapeutic drug monitoring. Pharm Res 2003; 20:1508–1513.